the $(12)^{-}$ state, which is only 50% larger than that for the $(02)^{-}$ state and a factor of 9 smaller than that for the $(03)^{-}$ state [in good agreement with the work of Sinha *et al.* (*16*)]. It is encouraging that, albeit several years after the experiments were performed, direct reliable comparison of theory with these experiment is possible.

In comparing all of the above theoretical and experimental results, it is worthwhile to keep in mind the very different sources of error in each case. The thermal rate coefficient for reaction 3 is, in one sense, both the most difficult to calculate theoretically and the simplest to measure experimentally. The theory is difficult because only with very large basis sets and very high level treatments of electron correlation can ab initio quantum chemistry provide a barrier height for these reactions that is accurate to within ~1 to 2 kJ mol^{-1}. The quantum dynamics calculation is also made more difficult by the fact that the thermal rate coefficient is dominated by contributions from vibrationally excited states of the reactants, requiring a large vibrational basis and separate calculations for many initial states. Achieving agreement for this seemingly mundane quantity to within ~35% is a substantial achievement for theory.

On the other hand, the theoretical calculation of the integral cross sections for reactions 1 and 2 (for near–ground state reactants at translational energies well above the barrier height) is relatively much easier. Given the accuracy of theory for the thermal rate coefficient, these integral cross sections may be seen to represent a more stringent test of experiment than of theory. The excellent agreement between the present results and experiments for reaction 1 illustrates the accuracy of our calculation in regard to the exchange region of the PES and the accuracy of the experimental measurement of absolute intensities. Unfortunately, the experimental cross sections for reactions 2 and 3 are completely inconsistent with our calculation and are seemingly inconsistent with the observed thermal rate coefficient. This is a case where the error anticipated for the theoretical result is relatively small. Reexamination of this experiment is therefore important, either to correct the presently accepted experimental results or to reveal the existence of some hitherto unsuspected problem with the theoretical calculations. Finally, it is particularly interesting to observe the huge difference in theoretical cross sections for the exchange and abstraction reactions shown in Figs. 2 and 3, although the barrier heights for these two reactions are coincidentally very close. This is the very effect of dynamics.

References and Notes

1. J. C. Polanyi, *Acc. Chem. Res.* **5**, 161 (1972).
2. G. C. Schatz, *J. Phys. Chem.* **100**, 12839 (1996).
3. D. C. Clary, *Science* **279**, 1879 (1998).
4. W. H. Miller, *Annu. Rev. Phys. Chem.* **41**, 245 (1990).
5. D. Neuhauser *et al.*, *Science* **257**, 519 (1992).
6. J. M. Bowman, G. C. Schatz, *Annu. Rev. Phys. Chem.* **46**, 169 (1996).
7. D. H. Zhang, J. Z. H. Zhang, *J. Chem. Phys.* **99**, 5615 (1993).
8. D. H. Zhang, J. C. Light, *J. Chem. Phys.* **104**, 4544 (1996).
9. D. H. Zhang, S. Y. Lee, *J. Chem. Phys.* **110**, 4435 (1999).
10. M. J. T. Jordan, K. C. Thompson, M. A. Collins, *J. Chem. Phys.* **102**, 5647 (1995).
11. K. C. Thompson, M. J. T. Jordan, M. A. Collins, *J. Chem. Phys.* **108**, 8302 (1998).
12. R. P. A. Bettens, M. A. Collins, *J. Chem. Phys.* **111**, 816 (1999).
13. M. A. Collins, D. H. Zhang, *J. Chem. Phys.* **111**, 9924 (1999).
14. R. P. Bettens, M. A. Collins, M. J. T. Jordan, D. H. Zhang, *J. Chem. Phys.* **112**, 10162 (2000).
15. A. Sinha, M. C. Hsiao, F. F. Crim, *J. Chem. Phys.* **92**, 6333 (1990).
16. ______, *J. Chem. Phys.* **94**, 4928 (1991).
17. F. F. Crim, *J. Phys. Chem.* **100**, 12725 (1996).
18. ______, *Acc. Chem. Res.* **32**, 877 (1999).
19. M. J. Bronikowski, W. R. Simpson, B. Girad, R. N. Zare, *J. Chem. Phys.* **95**, 8647 (1991).
20. ______, *J. Phys. Chem.* **97**, 2204 (1993).
21. R. N. Zare, *Science* **279**, 1875 (1998).
22. G. Hawthorne, P. Sharkey, I. W. M. Smith, *J. Chem. Phys.* **108**, 4693 (1998).
23. P. W. Barnes, P. Sharkey, I. R. Sims, I. W. M. Smith, *Faraday Discuss.* **113**, 167 (1999).
24. J. V. Michael, J. W. Sutherland, *J. Phys. Chem.* **92**, 3853 (1988).
25. K. Kleinermanns, J. Wolfrum, *Appl. Phys. B* **34**, 5 (1984).
26. S. Koppe, T. Laurent, P. D. Naik, H. Volpp, J. Wolfrum, *Can. J. Chem.* **72**, 615 (1994).
27. A. Jacobs, H. R. Volpp, J. Wolfrum, *J. Chem. Phys.* **100**, 1936 (1994).
28. R. A. Brownsword *et al.*, *Chem. Phys. Lett.* **259**, 375 (1996).
29. R. A. Brownsword *et al.*, *J. Phys. Chem.* **101**, 6448 (1997).
30. S. P. Walch, J. T. H. Dunning, *J. Chem. Phys.* **72**, 1303 (1980).
31. G. C. Schatz, H. Elgersma, *Chem. Phys. Lett.* **73**, 21 (1980).
32. D. C. Clary, *J. Phys. Chem.* **98**, 10678 (1994).
33. M. Alagia *et al.*, *Chem. Phys.* **207**, 389 (1996).
34. G. O. de Aspuru, D. C. Clary, *J. Phys. Chem.* **102**, 9631 (1998).
35. G. C. Schatz, G. Wu, G. Lendvay, D.-C. Fang, L. B. Harding, *Faraday Discuss.* **113**, 151 (1999).
36. We use the quadratic configuration interaction treatment with all single and double excitations and perturbative account of triple excitations [QCISD(T)], together with a reasonably large basis set with additional "diffuse" basis functions [6-311++G(3df,2pd)].
37. N. Cohen, K. Westberg, *J. Phys. Chem.* **83**, 46 (1979).

38. This work is supported in part by academic research grant RP3991603 from the National University of Singapore.

26 July 2000; accepted 21 September 2000

A Light-Emitting Field-Effect Transistor

J. H. Schön,* A. Dodabalapur,* Ch. Kloc, B. Batlogg

We report here on the structure and operating characteristics of an ambipolar light-emitting field-effect transistor based on single crystals of the organic semiconductor α-sexithiophene. Electrons and holes are injected from the source and drain electrodes, respectively. Their concentrations are controlled by the applied gate and drain-source voltages. Excitons are generated, leading to radiative recombination. Moreover, above a remarkably low threshold current, coherent light is emitted through amplified spontaneous emission. Hence, this three-terminal device is the basis of a very promising architecture for electrically driven laser action in organic semiconductors.

Field-effect transistors (FETs) are generally unipolar devices and minority carrier effects are negligible. However, ambipolar FETs, which operate as either n- or p-channel devices, depending on the polarity of the gate bias, can operate in a mixed or bipolar mode, in which both electron and hole currents are injected into the device at separate electrodes. Ambipolar FETs have been realized with amorphous silicon (*1*, *2*), organic semiconductor heterostructures (*3*), and organic single crystals (*4*, *5*). The formation of ohmic source and drain contacts and the use of a high-quality gate insulator are essential for the fabrication of such devices in order to ensure good charge transport for electrons and holes. Equal injection of electron and hole currents can be achieved in such devices by adjusting gate-source voltages (V_g) and drain-source voltages (V_d) (*6*). This leads to the formation of a pn-junction within the device, and consequently the generation of excitons might be expected. Although the use of such devices as light emitters has been proposed (*7*), no light emission has been reported from any kind of single FET device. We recently demonstrated ambipolar transistor action in the organic semiconductor α-sexithiophene (α-6T) (*5*), a material known to exhibit a reasonably high electroluminescence yield (*8*). Electron and hole mobilities as high as 0.7 and 1.1 $cm^2\ V^{-1}\ s^{-1}$ at room temperature have been observed in the high-temperature (HT) polymorph of this organic semiconductor. In addition, there have been reports of optically pumped lasing in sexithiophene (*9*) or related oligothiophene single

Lucent Technologies, Bell Laboratories, Murray Hill, NJ 07974, USA.

*To whom correspondence should be addressed. E-mail: hendrik@lucent.com; ananth@lucent.com

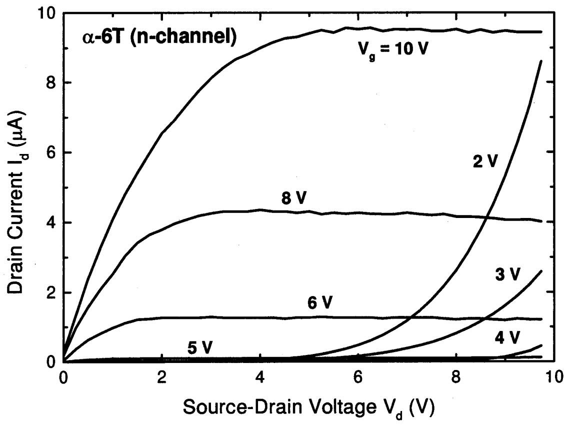

Fig. 1. Drain current of an ambipolar α-6T FET at room temperature as a function of positive drain-source V_d bias for different gate-source voltages V_g. At high gate voltage, the electron current dominates, whereas hole conduction becomes noticable at low gate and high source-drain voltages.

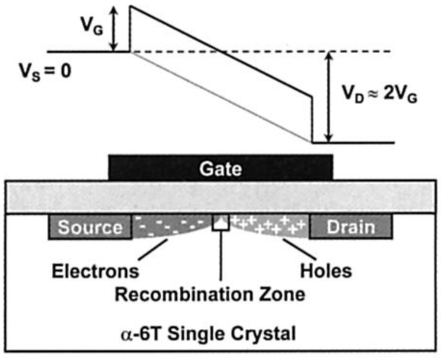

Fig. 3. Schematic picture of an ambipolar FET under balanced electron and hole injection ($V_d \approx 2V_g$). Whereas electrons are accumulated near the source electrode, the negative gate bias with respect to the drain results in the accumulation of positive charge carriers close to the drain region. For clarity, the dimensions are not to scale. The actual thicknesses of the crystal, the gate oxide, and the conducting channel are approximately 2 μm, 200 nm, and a few nanometers, respectively.

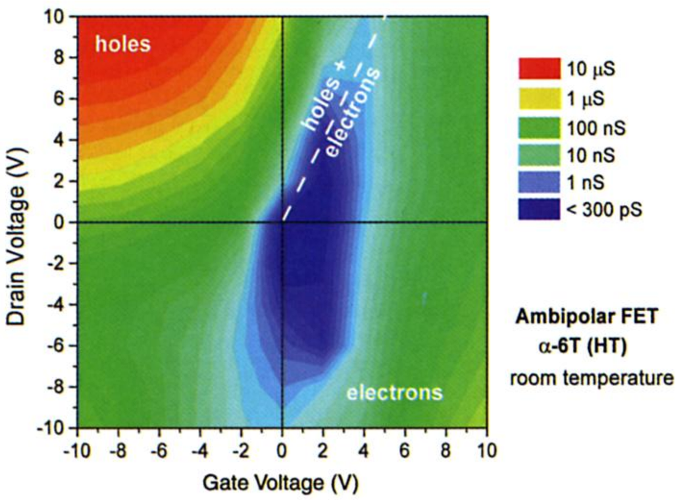

Fig. 2. Color plot of the channel conductivity of an ambipolar α-6T FET as a function of gate-source and drain-source bias on a logarithmic scale. The dashed line corresponds to more or less balanced electron and hole currents ($V_d \approx 2V_g$).

crystals (*10*). Therefore, this class of materials is a very promising choice for organic optoelectronic devices. Here we report on the preparation of a light-emitting transistor (LET) based on a single-crystalline, ambipolar α-6T (HT) FET. With this device, electrically driven amplified spontaneous emission was observed at high excitation levels. Threshold currents for the onset of stimulated emission were a few tens of microamperes.

Single crystals of α-6T (HT) were grown from the vapor phase in a flow of hydrogen (*11*). The material was slightly p-type, with a carrier concentration in the range of 10^7 cm^{-3}. FET structures were prepared using evaporated aluminum drain and source contacts (with a channel length and width of 25 and 750 μm, respectively), a sputtered Al_2O_3 gate insulating layer, and an Al-doped ZnO gate electrode (*4*, *5*). The contact for electrons was expected to be ohmic. There was a small barrier for the injection of holes. This can be reduced by biasing the device so that hole injection does not take place under saturation. In the transistor characteristics at room temperature for n-channel operation (positive V_g and V_d) (Fig. 1), typical FET curves were observed for large values of V_g, but unusual characteristics were seen for low V_g. The drain current strongly increased for low V_g and high V_d, which can be explained by the contribution of gate-induced holes in the channel. Electron and hole mobilities of 0.7 and 1.1 cm^2 V^{-1} s^{-1} were measured at room temperature with standard FET equations. At low temperatures, mobilities in the range of 200 cm^2 V^{-1} s^{-1} were achieved, demonstrating the high quality of the material.

The conductivity of the channel as a function of the applied bias on a color map with a logarithmic scale (Fig. 2) for positive V_d and negative V_g is given by holes in the FET channel, whereas electrons dominate for positive V_g and negative V_d. However, the electron and hole currents can be adjusted by the ratio of V_g and V_d in the other two quadrants (*1*, *2*, *6*). Assuming similar mobilities for both types of charge carriers, as in the case of α-6T, more or less balanced electron and hole injection is found at a gate bias of $V_g \approx \frac{1}{2}V_d$, which is high compared to the threshold voltages for n- or p-channel activity. This situation is depicted in Fig. 3. In the case of a positive gate bias, electrons are accumulated near the source electrode. However, close to the drain region, the gate bias with respect to the drain is negative, resulting in the accumulation of positive charge carriers. Consequently a pn-junction is formed in the channel region of the transistor. The two carrier types flow toward each other, excitons are generated, and radiative emission from the transistor is observed (Fig. 4). Hence, the FET works as an LET.

In the emission spectrum (Fig. 4), the three bands are ascribed to vibronic side bands (optical transitions with simultaneous phonon emission) of the transition between the lowest excitonic level and the ground state (*12*). The measurements were performed at room temperature in a He ambient. At high excitation currents, a significant narrowing of the first emission band (yellow, around 2.09 eV) was observed. We used pulsed electrical excitation (10 μs, 100 Hz, $V_d \approx 2V_g$) with currents up to 500 μA ($V_g \approx 50$ V). This corresponds to a carrier density in the channel region up to 10^{13} cm^{-2}. Upon increase of the drive current, the emission linewidth collapsed from 100 meV to less than 9 meV (Fig. 5), and the optical power rapidly rose beyond a threshold of approximately 20 μA (Fig. 5). This behavior is typical for amplified spontaneous emission. A change in the emission pattern was also observed.

The observation of amplified spontaneous emission can be seen as a result of a number of favorable factors, such as balanced electron and hole injection in the ambipolar FET and tight confinement of excitons in two dimensions. The multilayer structure shown in Fig. 3 also constitutes a multimode waveguide. The higher refractive index of ZnO (1.98) as compared to that of Al_2O_3 (1.7) and that of the organic semiconductor (~1.8) means that at low injection levels, the guided modes were concentrated in the ZnO layer. At higher injection levels, optical gain is expected to cause gain-guiding effects to dominate.

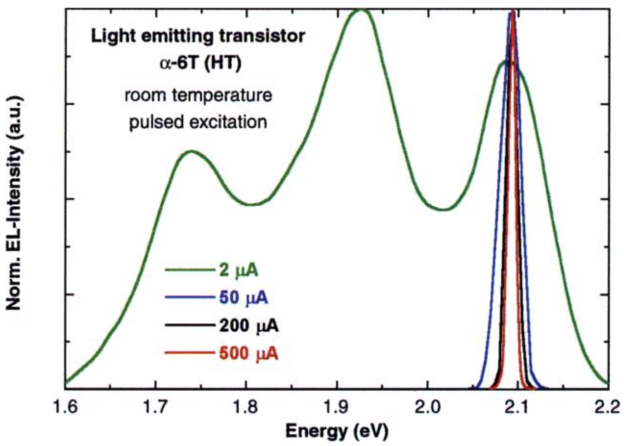

Fig. 4. Electroluminescence (EL) of an ambipolar α-6T single-crystal FET at room temperature for various currents under pulsed excitation. A strong narrowing of the emission due to amplified spontaneous emission is clearly observable with strong electrical excitation. The emission efficiency of the device can be estimated to be >1%.

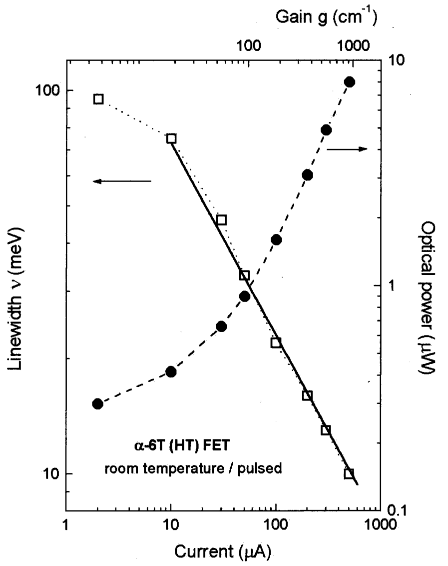

Fig. 5. Linewidth of the emission and optical power as a function of current. The linewidth estimated using a model for a 1D amplifier is also shown as a solid line [$\nu(0) \approx 110$ meV]. The estimated gain g is also indicated (upper scale).

The recombination zone, which constitutes the gain region, is spatially restricted by electrostatic effects and the diffusion length of excitons in organic semiconductors. It is appropriate to consider this device, from the optical standpoint, as a one-dimensional (1D) optical amplifier. Yariv *et al.* have derived a simple analytical expression for the linewidth of a homogenously broadened emitter as a function of optical gain when configured as a 1D amplifier (*13*). They obtained $\nu(I) = \nu(0)(\ln 2/g(I)z)^{0.5}$, where $\nu(I)$ is the linewidth at injection intensity I, $g(I)$ is the gain at intensity I (assuming $g \propto I$), and z is the length of the amplifier (750 μm). The calculated gain is shown as the solid line in Fig. 5. It can be seen that the functional form ($\nu \propto I^{-0.5}$) for the variation of linewidth with excitation intensity calculated by Yariv *et al.* agrees well with the experimental data.

The device structure shown in Fig. 3 also possesses favorable thermal properties. The thermal conductivity of most organic materials is low, and heat dissipation in lasers is obviously a major concern. In this structure, power dissipation occurs everywhere in the channel whereas the gain is confined to a small part of the channel. This is advantageous both for power dissipation and for achieving stimulated emission at low thresholds. This favorable situation has been achieved without expensive lithography or any etching of the semiconductor. The threshold current for observing the effects of optical gain is very small: about 20 μA. This is comparable to the threshold currents of the very best III-V semiconductor-based vertical cavity surface-emitting lasers (*14*), which are much smaller in size. Given the novel device geometry, it is worthwhile to define the threshold current density in specific ways. The effective threshold current density (current/channel area) is <1 A/cm^2. To the best of our knowledge, this is the lowest threshold current density (for stimulated emission) achieved in any material system at room temperature. However, the electrical threshold current density (current/channel cross section) is in the range of kA/cm^2, which is similar to electrically driven stimulated emission in tetracene (*15*). Another feature of this device is that the excitons are formed in a region where the electric field is close to zero.

We are encouraged that the maximum gain achieved (~900 cm^{-1}) is about one order of magnitude more than the system loss (estimated to be on the order of 100 cm^{-1}). Previous work on photoexcited organic lasers has shown that the threshold for laser action in distributed Bragg reflector (DBR) lasers is slightly lower than that for stimulated emission in an unpatterned planar waveguide (*16*). We expect, therefore, that it will be possible to realize DBR lasers with organic FETs by incorporating a grating in the structure. Many schemes have been demonstrated for the fabrication of such gratings (*17*). It may also be possible to include 2D photonic crystal–based couplers in order to couple light vertically out of the device (*18*).

The device structure allows for relatively simple pulsed operation because it is only necessary to apply a voltage pulse to the gate. The device structure is also suitable for integrating emissive devices with control devices, which perform switching functions. For such drive transistors, the ohmic contact could be formed with a low-workfunction metal. The Schottky barrier for hole injection will result in predominantly unipolar n-channel operation. Thus, essentially the same three-terminal device can double as a switching transistor and a laser. Moreover, this device architecture is also compatible with crystalline films of organic semiconductors, which can be grown on flexible plastic substrates. It has been recently demonstrated that films of pentacene grown on polyimide substrates possess high mobilities for holes and electrons (*5*). The development of other organic semiconductors, such as α-6T or tetracene, with good electrical and optical properties will facilitate the realization of low-cost, large-area organic semiconductor lasers. In addition, this device structure, which requires no intentional doping, could be useful in realizing laser action in material systems, which are difficult to dope.

References and Notes

1. H. Pfleiderer, *IEEE Trans. Electron. Devices* **ED-33**, 145 (1986).
2. G. W. Neudeck, H. F. Bare, K. Y. Chung, *IEEE Trans Electron. Devices* **ED-34**, 344 (1987).
3. A. Dodabalapur, H. E. Katz, L. Torsi, R. C. Haddon, *Science* **269**, 1560 (1995).
4. J. H. Schön, S. Berg, Ch. Kloc, B. Batlogg, *Science* **287**, 1022 (2000).
5. J. H. Schön, Ch. Kloc, B. Batlogg, in *Proceedings of the European Materials Research Society Spring Meeting*, May/June 2000, Strasbourg, France, in press.
6. A. Dodabalapur, H. E. Katz, L. Torsi, R. C. Haddon, *Appl. Phys. Lett.* **68**, 1108 (1996).
7. A. Dodabalapur, H. E. Katz, L. Torsi, *Adv. Mater.* **10**, 853 (1996).
8. G. Horowitz *et al.*, *Adv. Mater.* **6**, 752 (1994).
9. F. Garnier *et al.*, *Appl. Phys. Lett.* **72**, 2087 (1998).
10. D. Fichou, S. Delysse, J.-M. Nunzi, *Adv. Mater.* **9**, 1178 (1997).
11. Ch. Kloc, P. G. Simpkins, T. Siegrist, R. A. Laudise, *J. Cryst. Growth* **182**, 416 (1997).
12. M. Muccini *et al.*, *J. Chem. Phys.* **108**, 7327 (1998).
13. L. W. Casperson, A. Yariv, *IEEE J. Quantum Electron.* **8**, 80 (1972).
14. Z. Zou, D. L. Huffaker, D. G. Deppe, *IEEE Photon. Technol. Lett.* **12**, 1 (2000).
15. J. H. Schön, Ch. Kloc, A. Dodabalapur, B. Batlogg, *Science* **289**, 589 (2000).
16. M. Berggren, A. Dodabalapur, R. E. Slusher, Z. Bao, *Nature* **389**, 466 (1997).
17. J. A. Rogers, M. Meier, A. Dodabalapur, *Appl. Phys. Lett.* **74**, 3257 (1999).
18. A. Mekis, A. Dodabalapur, R. E. Slusher, J. D. Joannopoulos, *Opt. Lett.* **25**, 942 (2000).

19. We thank Z. Bao, F. Capasso, E. A. Chandross, S. V. Frolov, H. E. Katz, and R. E. Slusher for many helpful discussions.

11 August 2000; accepted 18 September 2000